

Investigation the Effect of Various Loads of Organically Modified Montmorillonite on Dyeing Properties of Polypropylene Nanocomposites

Maryam Ataefard,¹ Siamak Moradian²

¹Department of Printing Science and Technology, Institute for Color Science and Technology, Tehran, Iran

²Faculty of Polymer and Color Engineering, Amirkabir University of Technology, Tehran, Iran

Received 30 October 2010; accepted 27 April 2011

DOI 10.1002/app.34812

Published online 31 December 2011 in Wiley Online Library (wileyonlinelibrary.com).

ABSTRACT: Polypropylene (PP) nanocomposites having five different loadings of an organically modified montmorillonite, mineral clay was prepared by a melt mixing technique. The resultant PP nanocomposites were then uniformly dyed using three distinct disperse dyestuffs each at three concentrations. The enhanced dyeability of PP nanocomposite was characterized by spectrophotometric measurements. Good wash fastnesses were obtained after subsection of dyeing to a reduction clear process. It was found that increasing the clay content had a significant effect on dye uptake. Tensile strength tests showed improvements in mechanical properties. Degree of crystallinity of nanocom-

posites at various nanoclay loadings were investigated using differential scanning calorimeter. Surface behaviors of the resultant nanocomposites as well as the extent of exfoliation and dispersion of the nanoclay particles in PP were studied by various analytical techniques such as polarized optical microscope, X-ray diffraction, and transmission electron microscopy analytical techniques. These showed intercalate/exfoliate structures in the resultant nanocomposites. © 2011 Wiley Periodicals, Inc. *J Appl Polym Sci* 125: E214–E223, 2012

Key words: nanocomposite; polypropylene; nanoclay; dyeability; disperse dyestuffs; montmorillonite

INTRODUCTION

Polypropylene (PP) is a versatile, cheap, and widely used synthetic polymer¹ with several inherent advantages such as, high strength, high toughness, and resistance to chemicals.^{1–3} Its low cost and such mentioned properties make PP find a broad spectrum of use in industrial and home furnishing sectors.¹ However, PP does not enjoy comparable popularity in the apparel sector of the textile industry, the main reasons being its low moisture regain and lack of dyeability.^{1,3} Inability of PP to be colored by conventional dyeing techniques used for other is attributed to its high crystallinity, non-polar aliphatic structure,^{1,4} lack of functional groups to interact with dye molecules,⁵ and limited internal volume accessible to dye molecules.⁴ Therefore, the majority of commercially available PP is colored by mass pigmentation.^{1,6} Though the mass coloration procedures produce deep stable colorings which are economical for long run productions, but they suffer flexibility for short run productions. Limited numbers of shades, which additionally lack high chroma colors, and inability of shades to easily be corrected by redyeing and hence unsuitability for apparel wear

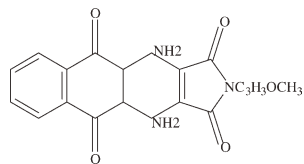
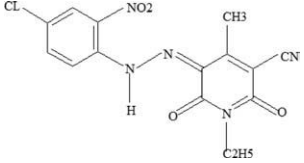
are also further disadvantages of the mass coloration procedures.^{1,5–11}

Modification of PP could impart new properties to this polymer. Many procedures have been used in the past to modify PP to enhance its affinity for Particular dyestuffs.^{7–11} Modification methods can be divided into two groups: chemical treatments, in which the polymer structure is chemically altered, and infusion treatments, in which foreign materials are infused into the fiber to impart hydrophilicity to act as dye receptor sites and/or enhance molecular diffusion within the PP matrix.^{4,12–16}

Polymer-layered silicate (PLS) nanocomposites exhibit outstanding improvements in material properties when compared with neat and conventional micro-, macrocomposites.¹ The enhancements in properties include reinforced mechanical properties,^{1,2} better thermal resistance,^{17–21} reduced gas permeability,^{22–24} improved solvent resistance,^{25–27} enhanced ionic conductivity,²⁶ etc. Montmorillonite, a clay mineral, is the most widely used filler for preparing PLS nanocomposites.² Exchanging the interlaminar cations with organic cations can alter the surface chemistry of montmorillonite.¹ Nanotechnology has been used to increase tensile strength, flexural modulus, and heat resistance of polymeric materials.⁸ It has also recently been reported that PP matrices can be dyed by incorporation of such nanoclays.^{1–4}

Correspondence to: S. Moradian (moradian@aut.ac.ir).

TABLE I
Generic and Commercial Names of Three Disperse Dyestuffs

Commercial name	Generic name	Chemical structure	Chemical structure	Activation energy
Terasil blue BG	C.I. Disperse blue 60	Anthraquinone		Medium
Terasil yellow 4G	C.I. Disperse yellow 211	Pyridine		Medium
Terasil red R	C.I. Disperse red 324	Mono azo		Medium

PP homopolymers are not capable of intercalating between organoclay layers because they are not polar enough to interact with such modified layers. However, a compatibilizer could be used to improve clay dispersion within PP and facilitate subsequent exfoliation of the clay platelets. Majority of studies had used a more polar maleated PP (PP-MA) as a compatibilizer for such purposes. PP/nanoclay nanocomposites (PPNC), prepared by either conventional intensive shear mixing or twin screw extrusion, have been successfully produced.¹² In the present study, the enhancement of the dyeability of a three component mixture of PP/PP-MA/Closite 15A was sought after.

EXPERIMENTAL

Materials

Closite 15A, an organically modified montmorillonite nanoclay supplied by Southern Clay Products (USA), was used as received to prepare a series of three component PP/PP-MA/nanoclay hybrids. PP (grade V30S) was supplied by Arak Petrochemical Company (Iran). PP-MA grade Fusabond P MD353D was supplied by DuPont Company (USA). Three disperse dyestuffs (a yellow, a red, and a blue) was supplied by Ciba Company (Switzerland) Iran Branch.

Preparation of nanocomposites

Nanocomposites were prepared by melt mixing the three components in an internal mixer. Various clay concentrations, namely, 1%, 3%, 5%, 7% and 10% by weight of PP, were used in such a way that the ratio of nanoclay : PP-MA was always 1 : 1. Such nanocomposites were then named as PP1, PP3, PP5, PP7, and PP10. Polymer melt-direct intercalation was the

approach for making PLS nanocomposites using a conventional Brabender PL2000 plasticorder melt mixer (Germany). The variable parameters of such a mixer were set at a screw speed of 60 rpm at a temperature of 180°C for a time of 15 min. Nanocomposite films of 300 μm thickness were subsequently prepared by a Carver laboratory press (Germany) at a pressure of 100 bar and a temperature of 190°C.

Dyeing

The resultant PP nanocomposites coded as PP1–PP10 signifying PP containing various loads of 1–10% of Closite 15A, and a corresponding amount of PP-MA was then dyed to four depths of shades, namely 0.5%, 1%, 3%, and 5% on the weight of the prepared films. For comparison purposes, virgin PP (PP0) and virgin polyester (PET0) were also dyed with the same dyestuffs at the same concentrations using the same dyeing procedure. The commercial dyes were used without any purification and are listed in Table I. The dyeing procedure was a semi-conventional technique used for dyeing polyester at 100°C without any carriers, the liquor to goods ratio was 100 : 1. A pH of 5.5 was reached in each dye bath by adding 3% owf of acetic acid supplied by Merck company (Germany). A 1 gl^{-1} of the dispersing agent Invalon HTB, supplied by Ciba company (Switzerland) Iran Branch, was also added to each dye bath. Dyeing was performed by raising the initial temperature (40°C) to a final temperature (100°C) at a rate of 2°C min^{-1} , and holding at 100°C for 60 min.

A subsequent reduction clear procedure was performed on each sample after dyeing. This comprised of treating each sample in a solution of 2 gl^{-1} sodium hydroxide supplied by Ciba Company (Switzerland) Iran Branch, and 3 gl^{-1} sodium hydrosulfite also

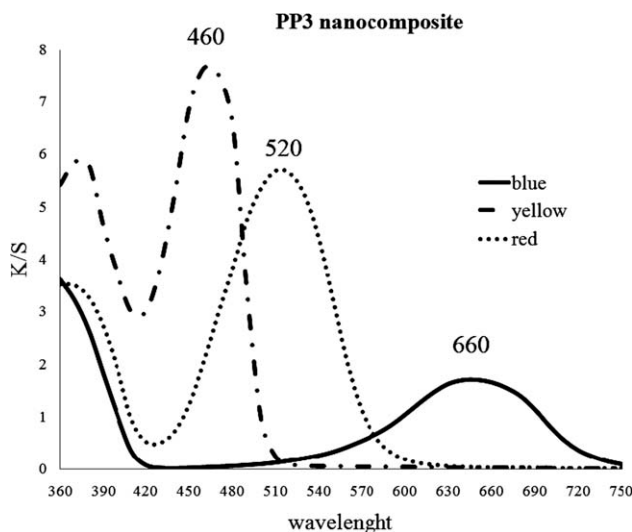


Figure 1 Variations of K/S values of three disperse dyes for the PP3 nanocomposite.

supplied by the same company carried out at 70°C for 20 min. The samples were then rinsed in cold water.

Characterization of the nanocomposites

Spectrophotometric measurements

Reflectance values of all dyed nanocomposites and their respective controls were obtained using a Macbeth Color Eye 7000A spectrophotometer (Gretag Macbeth Company (USA)). The samples were all mounted on the same white background, and the specular-in-mode was selected for all measurements. All measurements were carried out on five different positions of each sample, and the average value was reported.

The K/S values of all samples were calculated using the Kubelka–Munk one constant theory. The

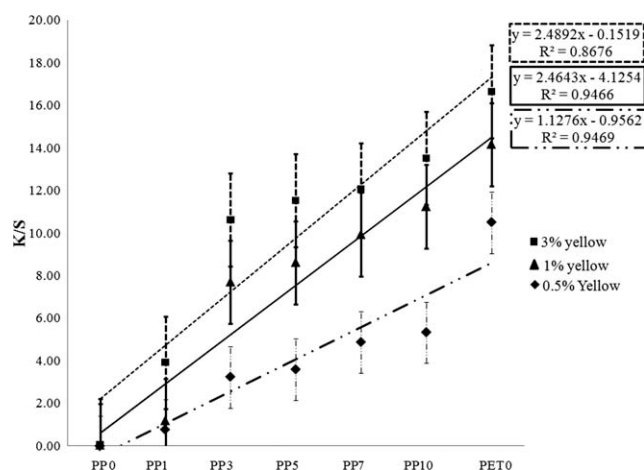


Figure 2 Color build-up curves of C.I. Disperse yellow 211 at three concentrations for various PP nanocomposites PP1 to PP10. PP0 and PET0 are similar dyeing of neat PP and neat PET, respectively.

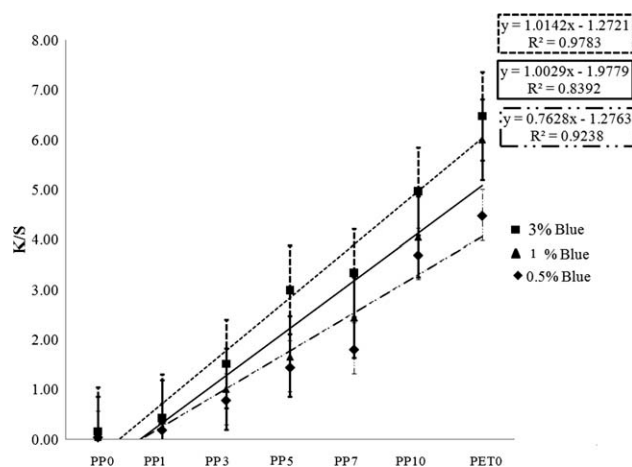


Figure 3 Color build-up curves of C.I. Disperse blue 60 at three concentrations for various PP nanocomposites PP1 to PP10. PP0 and PET0 are similar dyeing of neat PP and neat PET, respectively.

corresponding K/S values at wavelength of maximum absorption are shown in Figure 1 and are indicative of color yields of the chosen dyestuffs on dyed PP nanocomposites.

The Kubelka–Munk K/S values were calculated by the aid of eq. (1):

$$K_{\lambda}/S_{\lambda} = (1 - R_{\lambda})^2 / (2 \times R_{\lambda}) \quad (1)$$

where K_{λ} is the absorption coefficient, S_{λ} is the scattering coefficient, and R_{λ} is the measured reflectance values at 10 nm intervals throughout the visible spectrum namely (360–750 nm). The corresponding color yields are shown in Figures 2–4 and Tables II–IV.

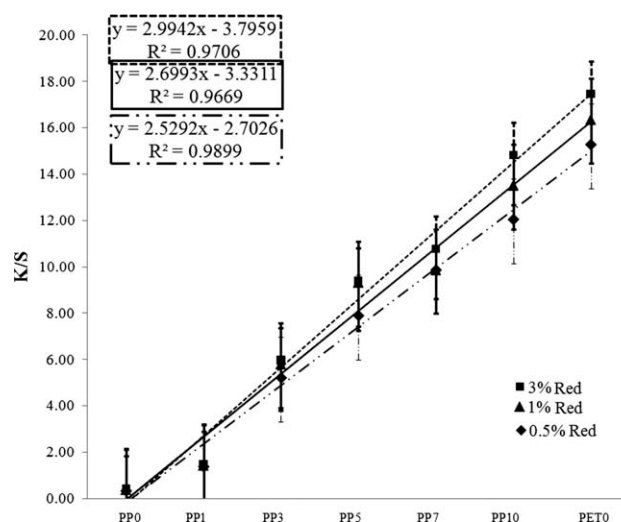


Figure 4 Color build-up curves of C.I. Disperse red 324 at three concentrations for various PP nanocomposites PP1 to PP10. PP0 and PET0 are similar dyeing of neat PP and neat PET, respectively.

TABLE II
Build-Up of C.I. Disperse Red 324 at 4% Concentrations (0.5, 1, 3, 5 owf) for Virgin PP0, Virgin PET0, and Various PP Nanocomposites Containing 1–10% Closite 15A

K/S values	Dyestuff concentration (owf)			
	0.5%	1%	3%	5%
PP0	0.32	0.39	0.42	0.17
PP1	1.36	1.44	1.48	1.79
PP3	5.20	5.81	5.97	5.63
PP5	7.88	9.33	9.41	9.25
PP7	9.85	9.87	10.77	9.90
PP10	12.03	13.52	14.82	13.14
PET0	15.26	16.35	17.46	18.77

Colorfastness tests

Color fastnesses of various dyed nanocomposites to washing and light were evaluated according to the ISO 105-C02:1989(E) and ISO 105-B02:1994(E), respectively. All colorfastness tests were performed on neat PP0 and PET0 as well as various PP nanocomposites and are shown in Tables V and VI.

X-ray diffraction

Wide-angle X-ray diffraction (XRD) was conducted at ambient temperatures on a Rigaku rotating-anode diffractometer with Cu radiation), at a wavelength of 1.54 Å supplied by Philips, X'Pert (Netherlands). The accelerating voltage was 40 KV. The montmorillonite clay particles, i.e., Closite 15A were measured in powder form, and the nanocomposites were studied in the form of opaque films. The results are shown in Figure 5 and Table VII.

Differential scanning calorimeter

Thermal analysis was carried out using a differential scanning calorimeter (DSC) DSC 60 supplied by Shimadzu company (Japan). Nitrogen gas was used to provide an inert atmosphere. The sample and reference pans were heated to 250°C and then cooled

TABLE III
Build-Up of C.I. Disperse Yellow 211at 4% Concentration (0.5, 1, 3, 5 owf) on Virgin PP0, Virgin PET0, and Various PP Nanocomposites Containing 1–10% Closite 15A

K/S values	Dyestuff concentration (owf)			
	0.5%	1%	3%	5%
PP0	0.01	0.03	0.04	0.15
PP1	0.79	1.18	3.92	3.09
PP3	3.27	7.70	10.63	9.56
PP5	3.62	8.62	11.87	11.54
PP7	4.90	9.94	12.06	11.56
PP10	5.36	11.25	13.52	12.93
PET0	10.54	14.17	16.66	17.62

at the rate of 10°C min⁻¹. The results are shown in Figure 6 and Table VIII.

Polarized optical microscopy

Polarized optical microscope (POM) model leica DMRX supplied by Linkam company (UK) was used to evaluate number and size of spherulites present in various nanocomposites. The results are shown in Figure 7 and Table IX.

Tensile Testing

Tensile testing of prepared nanocomposites and neat PP0 were carried out according to the ASTM standard test method D882 on an instron 5566 instrument supplied by Instron company (Italy) at crosshead speed of 5 mm min⁻¹. The results are shown in Table X.

TEM

The extents of intercalation and exfoliation of the clay were monitored by transmission electron microscopy (TEM), Philips CM 120 (Netherlands). The preparation of samples for TEM was carried out by the IBB laboratory of Tehran University (Iran). Samples were scanned by TEM at an accelerating voltage of 100 KV. Results are shown in Figure 8.

RESULT AND DISCUSSION

Build-up and fastness analysis

The dyeing behavior of a substrate depends on both its physical and chemical structure. Regarding chemical structure, dyeability is governed by the presence, first, of polar groups, which interact with water molecules and allow substrate swelling and, second, by functional groups, which attract dye molecules.³

Physical structure enables the substrate to be accessible to water, dyestuffs, and other reagents. Physically, the substrate must have certain permeability to

TABLE IV
Build-Up of C.I. Disperse Blue 60 at 4% Concentration (0.5, 1, 3, 5 owf) on Virgin PP0, Virgin PET0, and Various PP Nanocomposites Containing 1–10% Closite 15A

K/S values	Dyestuff concentration (owf)			
	0.5%	1%	3%	5%
PP0	0.04	0.04	0.16	0.14
PP1	0.18	0.38	0.42	0.51
PP3	0.78	1.01	1.51	1.75
PP5	1.44	1.66	2.89	2.99
PP7	1.80	2.44	3.34	4.37
PP10	3.69	4.05	4.96	5.74
PET0	4.48	6.01	6.47	6.53

TABLE V
Wash Fastness for Virgin PP0, Virgin PET0, and Various PP Nanocomposites Containing 1–10% Cloisite 15A for Three Disperse Dyestuffs at 1% Concentration

Sample	Staining (GSR)						Washed (GSR)		
	Acrylic	Polyester	Nylon	Acetate	Cotton	Wool	Blue	Yellow	Red
PP0	5	5	5	5	5	5	4–5	5	5
PP1	5	5	5	5	5	5	4–5	4–5	4–5
PP3	5	5	5	5	5	5	4–5	4–5	4–5
PP5	5	5	5	5	5	5	4–5	4–5	4–5
PP7	5	3–4	4–5	5	5	5	4–5	4–5	4–5
PP10	5	4–5	5	5	5	5	4–5	4–5	4–5
PET0	5	5	5	5	5	5	5	5	5

various reagents particularly it must permit dyestuffs molecules to diffuse into the substrate's matrix. In PP nanocomposites, the accessibility can be improved by the introduction of particulates into its matrix.²⁸

Three different possibilities could enhance dye-ability of PP nanocomposites:

1. Provision of sites within the bulk of nanocomposites capable of chemical and/or physical linkage to particular dyestuffs. Therefore, nanoclays should carry or be able to develop charged or other functional groups capable of interacting with certain dyestuffs.
2. Pores and cracks may develop on the surface and or the bulk of a nanocomposite during processing. Such submicroscopic voids may allow diffusion of dyestuffs into the nanocomposite.
3. Dye diffusion may occur through a wicking process.^{2,4}

All the above mentioned possibilities could synergistically combine to enhance dyeing of PP nanocomposites. The greater the compatibility of clay particles within the PP matrix, the greater the dispersion uniformity of nanoclays within such a matrix and consequently the better the dyeing properties of the resultant nanocomposite would be.

Secondary forces such as van der Waals forces may be active between disperse dye molecules and

clay particles, as well as between disperse dye molecules and modified PP matrix.

Figure 1 shows the variation of K/S with wavelength for three disperse dyestuffs on the PP3 nanocomposite. The build-up curves of disperse dyes are shown in Figures 2–4 and Tables II–IV. From build-up curves it is evident that a good correlation exists between the clay add-on and the dye sorption of the prepared nanocomposites. Results tend to suggest that by correct selection of dyestuffs, higher color yields could be obtained on such nanocomposites.

Wash fastness of dyestuffs is rated by two broad categories: (i) color change between washed and unwashed samples and (ii) color staining of adjacent substrates. Table V shows the gray scale rating (GSR) of both color change of dyed films and staining of various adjacent substrates. The washed disperse dyed samples showed little or no color change.

Light fastness assessed by the blue scale rating (BSR) of disperse dyestuffs on neat PP0 and its various nanocomposites is shown in Table VI. The chosen disperse dyestuffs, generally conferred poor light fastness results on PP nanocomposite fibers (Table VI). However, this is largely related to

TABLE VI

Light Fastness for Virgin PP0, Virgin PET0, and Various PP Nanocomposites Containing 1–10% Cloisite 15A for Three Disperse Dyestuffs at 1% Concentration

Sample	Light fastness (BSR)		
	Blue	Yellow	Red
PP0	–	–	1
PP1	2–3	1	1–2
PP3	2–3	1–2	2
PP5	2–3	2	2
PP7	3	4	2–3
PP10	3–4	4–5	2–3
PET0	6–7	6–7	6–7

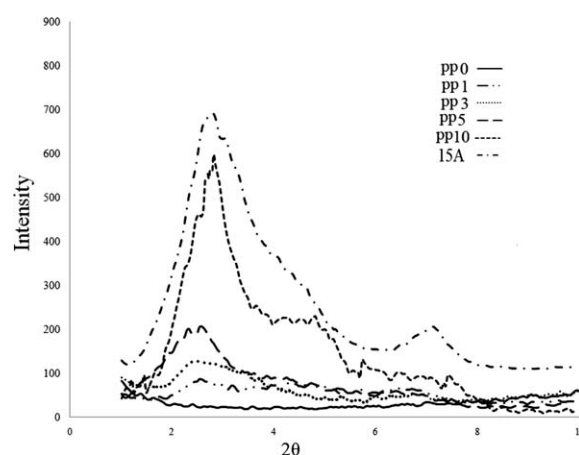


Figure 5 XRD micrographs for various PP nanocomposites PP1 to PP10. PP0 and Cloisite15A are for neat PP and nanoclay, respectively.

TABLE VII
XRD Parameters for Various PP Nanocomposites PP1 to PP10

Nanocomposite	<i>d</i> -Spacing	2θ	Δ
15A	3.10	2.76	–
PP0	–	–	0
PP1	3.65	2.40	0.55
PP3	3.56	2.50	0.46
PP5	3.44	2.57	0.34
PP10	3.29	2.68	0.19

PP0 and Cloisite15A are for neat PP and nanoclay, respectively.

whether the standard shades for lightness is reached or not. As it can be seen in nanocomposites having higher loads of nanocomposites (i.e., PP10) as a consequence of steadily approaching the standard shade, the light fastness of all three dyestuffs increases accordingly.

XRD analysis

XRD can be used to estimate the degree of dispersion of nanoclays within the PP matrix through obtaining the distance between individual platelets of nanoclay. A shift to lower angles of characteristic diffraction peak suggests an increase in interlayer spacing or gallery of the nanoclay, which is referred to as intercalation.¹² Disappearance of the nanoclays inter-

layer diffraction peak indicates possible exfoliation of the nanoclay platelets and broadening of the peak is considered to be the result of partial exfoliation. The XRD spectra of nanoclay and nanoclay/PP nanocomposites containing various loads of nanoclay are shown in Figure 5. The degree of dispersion was measured by calculating the *d*-spacing from Bragg's law [eq. (2)] and is depicted in Table VII.

$$n \cdot \lambda = 2d \sin \theta \quad (2)$$

where *n* is an integer, λ is the wavelength of a beam of the X-ray incident on a crystal with lattice planes separated by distance *d*, and θ is the Bragg angle.

Initially, the diffraction peak and *d*-spacing of the organically modified montmorillonite particles were observed. The peak of Cloisite 15A particles occurred at a 2θ value of 2.76, with a *d*-spacing of 3.1. Subsequently, this basal spacing (i.e., *d*001 value of 3.1 nm at diffraction peak 2θ = 2.76° for the Cloisite 15A particles) was compared with its corresponding changes in appropriate nanocomposites. No peaks occurred between 2θ values of 2–10° for PP0, and this demonstrated that the (*d*001) observed peaks at 2θ = 2–10° belonged only to the nanoclay particles.

The increased *d*-spacing in the resultant nanocomposites might be attributed to the presence of PP and/or PPM molecules within the nanoclay particles. Therefore, it is highly likely that during the

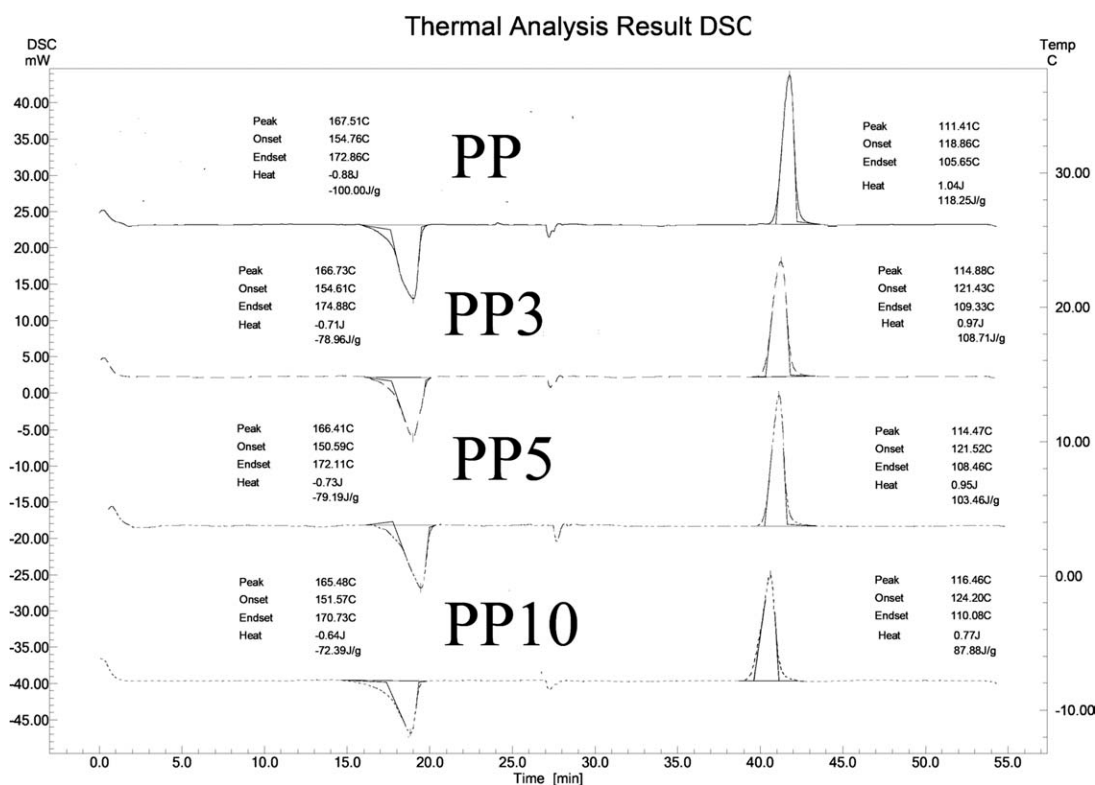


Figure 6 DSC thermal parameters for various nanocomposites PP3 to PP10. PP0 is for neat PP.

TABLE VIII
DSC Parameters for Various PP Nanocomposites PP1 to PP10

Nanocomposite	T_m	ΔH_m	T_c	ΔH_c	% crystallinity
PP0	168	-100	111	118	48.29
PP3	167	-79	114	109	38.13
PP5	166	-79.2	114	103	38.24
PP10	165	-72.4	116	87.9	34.95

PP0 is for neat PP.

formation of nanocomposites, PP and/or PPM molecules enter the galleries of the clay particles.

The XRD curves of nanocomposite showed a slight shift of the peak towards lower angles, thereby indicating that the distance between clay platelets had become greater. It seems that increased loads of nanoclay tend to reduce the enhanced d-spacing. Moreover, increased height of the peak in Figure 6 also shows that increased loads of nanoclay decreases the amount of exfoliated clay as does the d-spacing but at lower domains of exfoliated clay.^{25,29}

Results show that intercalation has occurred in all nanocomposites because all 2θ values are lower than the nanoclay itself. The extent to which the distance between platelets has increases can be estimated from the differences between the d-spacing of each

nanocomposite and the d-spacing of pure nanoclay; this difference Δ is also given in Table VII. Increased loads of nanoclay increases 2θ values, which indicate reduced distance between layered platelets of nanoclay. Table VII also illustrates the reduced d-spacing and the corresponding Δ values, however it must be noted that in all cases, the d-spacing is more than the nanoclay itself. Therefore, the Δ values are all positive. Increased loads of nanoclay increases the peak's heights in Figure 6, where the peak's height for the PP10 load almost reaches the peak height of the nanoclay itself. Lowered peak height for PP1 and PP3 loads of nanoclays are indicative of great extents of exfoliation of nanoclay in the PP matrix. The PP5 load of nanoclay can also be considered as an acceptable extent of exfoliation.

DSC analysis

DSC results (Figure 6 and Table VIII) showed that all nanocomposite films are less crystalline than the virgin PP0. It can therefore be argued that improved dyeability of nanocomposites could also be due to decreased crystallinity. However, decreased crystallinity of nanocomposites cannot be considered as the only reason for their high color yields. The melting point T_m decreased because increased

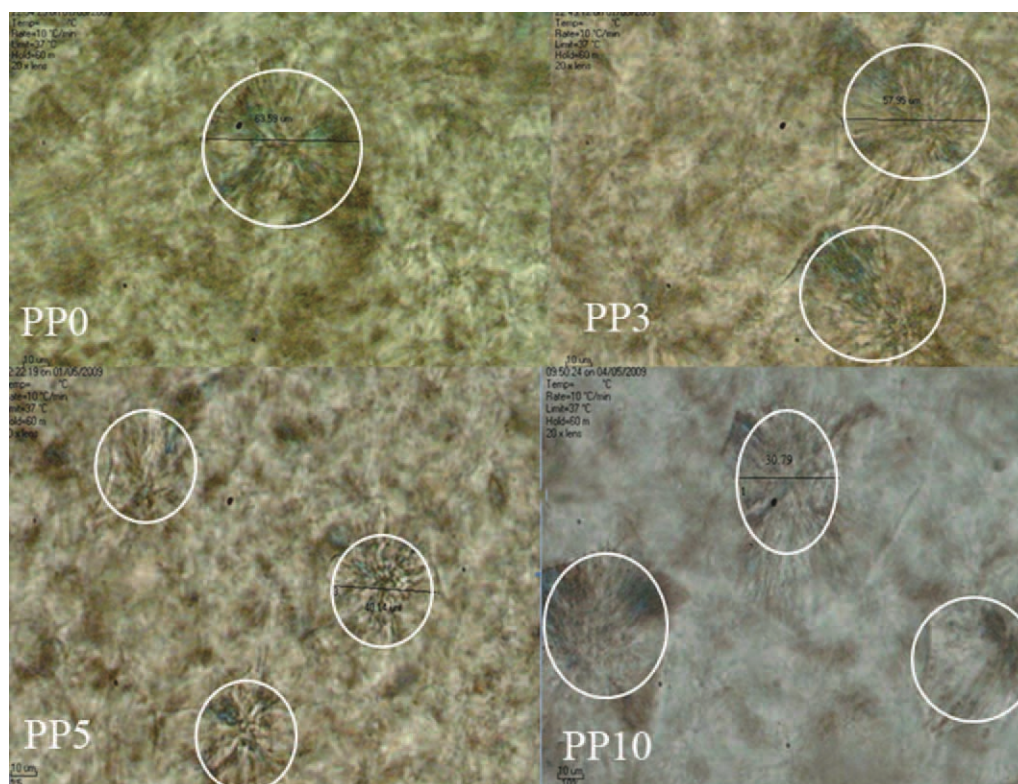


Figure 7 Polarized optical micrographs of size and number of spherulites for various nanocomposites PP3 to PP10. PP0 is for neat PP at the same magnification of 100. [Color figure can be viewed in the online issue, which is available at wileyonlinelibrary.com.]

TABLE IX
Spherulites Size of Various PP Nanocomposites PP1 to PP10

Nanocomposite	Spherulites size (μm)
PP0	63.59
PP3	57.95
PP5	40.14
PP10	30.79

PP0 is for neat PP as obtained from polarized microscopy.

interactions of nanoclay particles–PP matrix affect chain mobility.³⁰

The crystallization temperature T_c increased from 111°C for virgin PP0 to 116°C for the nanocomposite having the highest load of nanoclay. This increased crystallization temperature of PP could be attributed to nanoclay particles–PP matrix interactions together with the effect of nanoclay acting as a nucleating agent increasing the number of spherulites.³¹ Decreased differences in enthalpy of crystallization ΔH_c and enthalpy of melting ΔH_m are both indicative of reduced crystallinity.³²

The melting temperature T_m decreased as the content of nanoclay in the resultant nanocomposites increased. This can be attributed to enhanced motions of polymeric chains in the presence of nanoclay particles. Nanoclay particles cause restructuring of polymer chains, hence, decreasing the percent crystallinity. ΔH_c and ΔH_m confirmed this deduction. Reduction in crystallinity can by itself improve dyeability because dyeing mostly occurs through and in the amorphous regions. However, because the estimated reduction in crystallinity tended not to be very large therefore it is doubtful that it could be considered as the only deterministic parameter in dye uptake. Nanoclay particles, generally, act as nucleation sites for the formation of spherulites. Increased values of T_c illustrate increased numbers of such spherulites. However due to overall decrease in crystallinity the size of each spherulite must decrease. This subject was further investigated by POM.

TABLE X
Mechanical Properties of Various PP Nanocomposites PP1 to PP10

Nanocomposite	Young modulus (Mpa)	Stress (Mpa)	Strain (%)
PP0	850.25	20.02	6.33
PP1	981.25	21.79	4.54
PP3	1088.77	23.68	3.93
PP5	1138.41	26.22	3.83
PP7	1238.96	28.2	3.75
PP10	1249.45	32.44	3.5

PP0 is for neat PP.

Polarized optical microscopy

Polarized light micrographs of neat PP0 and PP–clay nanocomposites are depicted in Figure 7. The average spherulite's size was dramatically reduced on reinforcement of PP0 with the nanoclay (Table IX). This reduction in size is ascribed to the nucleating effect of clay. The decrease in spherulite size is caused by higher nucleation density induced by nanoclay particles. Such a conclusion was also arrived at from the DSC results mentioned above.²⁷

Optical microscopic images of Figure 7 illustrate that increased loads of nanoclay increase the number of spherulites however the dimension of each spherulite is decreased. Therefore, the overall percent crystallinity of nanocomposites decrease with increased loads of nanoclay. Table IX clearly illustrates that dimensions of spherulites has decreased with increased loads of nanoclay. Microscopic images of Figure 7 also clearly illustrate increased numbers of spherulites together with decreased sizes of each spherulite.

Tensile analysis

Table X shows some mechanical properties of virgin PP0 and its various nanocomposites. The results show increased modulus and breaking stresses for all nanocomposites compared with virgin PP0. However, the nanocomposites showed the reduction in

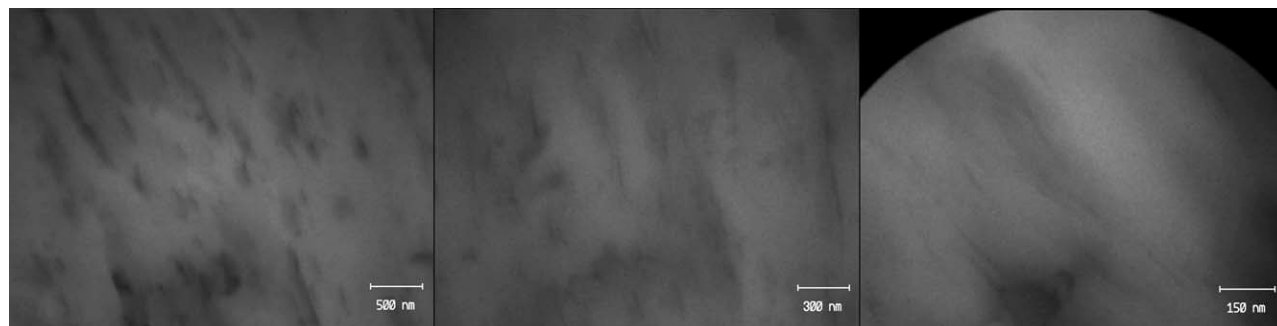


Figure 8 TEM micrographs of PP3 nanocomposites.

elongation at break compared with virgin PP0, such as enhancements in mechanical properties are in good agreement with other studies.²⁷ This infers that reinforcement of polymer chains with nanoclay platelets causes increased modulus and increased breaking stress of the resultant nanocomposites. However, the reinforcement of PP0 with nanoclay particles also causes restricted mobility of the polymer chains hence leading to reduced elongation at break of the nanocomposites. Another possible explanation for decreased elongation at break with simultaneous improvement in modulus and breaking stress of such nanocomposites could be increased viscosity of these nanocomposites with increased loads of nanoclay together with the concomitant increase in the orientation of the resultant nanocomposites.^{1,29}

Transmission electron microscopy

TEM is a commonly used technique for measuring clay dispersions. Figure 8 shows TEM micrographs of PP3 nanocomposites. For the PP/PP-MA/C15A composites, a uniform dispersion of the clay particles in the polymer matrix was observed. It was shown that exfoliation depends not only on maximization of favorable interactions between the polymer matrix and the organically modified silicate such as Lewis-acid/base interactions or hydrogen bonding but also on minimization of unfavorable interactions between the polymer matrix and the alkyl chains of the organic modifier, present on the silicate such as poor physical interactions.²⁶ This explains the need to utilize functionalized polymer with polar groups, such as PP-MA, to favor intercalation and exfoliation.³³ It has been well established that an intercalated/exfoliated structure is usually formed in a PP-nanoclay system by using PP-MA as a compatibilizer.^{25,26} However, the formation of a clay network depends on connecting clay layers and tactoids.

In the TEM images, some aggregations of nanoclay tactoids are also detectable, which indicate that degree of exfoliation in such PPNC synthesized via melt compounding is lower than polar polymer/nanoclay systems, such as nylon/nanoclay,³³ epoxy/nanoclay³³ nanocomposites, in which well-defined exfoliations of clay were frequently confirmed by XRD and TEM. The lower degree of exfoliation can be ascribed to the fact that chemical miscibility and interaction between PP chains and nanoclay particles are still weak compared with polar polymer-based nanocomposites even when a compatibilizer is incorporated. Therefore, TEM analysis provides complementary results to XRD and SEM analyses to validate the exfoliated/intercalated structures in such nanocomposites which are uniformly dispersed in the polymer matrix.^{26,33}

CONCLUSIONS

PP0 could be made dyeable by incorporating nanoclay particles. As compared with virgin PP0, high build-up uniformly dyed nanocomposites were observed with disperse dyestuffs. All PP nanocomposites exhibited better dye uptake than virgin PP0. The dyed nanocomposites exhibited excellent wash fastnesses and satisfactory light fastnesses.

Tensile testing of virgin PP0 and its nanocomposites with the chosen nanoclay showed that modification of PP0 with organically modified nanoclays containing quaternary ammonium groups increased the modulus and the strength of the resultant nanocomposites. However, such nanocomposites showed the reduction in elongation at break compared with virgin PP0.

DSC parameters showed that incorporation of nanoclays into the PP matrix decreased crystallization and lowered the melting point and increased the crystallization temperature. XRD showed increased d-spacing and a good deal of exfoliation.

SEM analyses showed homogeneous dispersions in morphologies of PP3 and PP5 nanocomposites but as expected, clay aggregates are more prevalent for the PP10 nanocomposite. Complementary results from TEM analyses qualitatively verified the previous findings from XRD and SEM analyses demonstrating intercalated/exfoliated nanocomposite structures.

References

1. Toshniwal, L.; Fan, Q.; Ugbolue, S. C. *J Appl Polym Sci* 2007, 106, 706.
2. Mani, G.; Fan, Q.; Ugbolue, S. C.; Yang, Y. *J Appl Polym Sci* 2005, 97, 218.
3. Razafimahefa, L.; Chlebicki, S.; Vroman, I.; Devaux, E. *Color Technol* 2008, 124, 86.
4. Dar, Y. S.; Fan, Q.; Ugbolue, S. C.; Wilson, A. R.; Yang, Y. *NSTI Nanotech Conference*, 2006.
5. Ahmed, M. *Polypropylene Fibers—Science and Technology*; Elsevier: New York, 1982.
6. Cook, J. C. *Handbook of Polyolefin Fibers*; Merrow Publishing: Watford, 1973.
7. Ujhelyiova, A.; Bolhova, E.; Oravkinova, J.; Tiño, R.; Marcinčin, A. *Dyes Pigments* 2007, 72, 212.
8. Burkinshaw, S. M.; Froehling, P. E.; Mignanelli, M. *Dyes Pigments* 2002, 53, 229.
9. Broda, J.; Gawłowski, A.; Slusarczyk, C.; Wlochowicz, A.; Fabia, J. *Dyes Pigments* 2007, 74, 508.
10. Tehrani, A. R.; Shoushtari, A. M.; Malek, R. M. A.; Abdous, M. *Dyes Pigments* 2004, 63, 95.
11. Seves, A.; De Marco, T.; Siciliano, A.; Martuscelli, E.; Marcandalli, B. *Dyes Pigments* 1995, 28, 19.
12. Tanuma, S.; Kamimura, H. *Graphite Intercalation Compounds*; World Scientific: Philadelphia, 1985.
13. Kawasumi, M.; Hasegawa, N.; Kato, M.; Usuki, A.; Okada, A. *Macromolecules* 1997, 30, 6333.
14. Akerman, J.; Prikyl, J. *J Appl Polym Sci*, 1996, 62, 235.
15. Razafimahefa, L.; Chlebicki, S.; Vroman, I.; Devaux, E. *Dyes Pigments* 2005, 66, 55.
16. Akerman, J.; Prikyl, J. *J Appl Polym Sci* 1999, 73, 719.

17. Usuki, A.; Kojima, Y.; Kawasumi, M.; Okada, A.; Fukushima, Y.; Kurauchi, T.; Kamigaito, O. *J Mater Res* 1993, 8, 1179.
18. Usuki, A.; Kojima, Y.; Kawasumi, M.; Okada, A.; Fukushima, A.; Kurauchi, T.; Kamigaito, O. *J Mater Res* 1993, 8, 1185.
19. Yano, K.; Usuki, A.; Okada, A.; Kurauchi, T.; Kamaigaito, O. *J Appl Polym Sci* 1993, 31, 2493.
20. Liu, L.; Qi, Z.; Zhu, X. *J Appl Polym Sci* 1999, 71, 1133.
21. Okamoto, M.; Nam, P. H.; Maiti, P.; Kotaka, T.; Hasegawa, N.; Usuki, A. *Nano Lett* 2001, 1, 295.
22. Nussbaumer, R. J.; Caseri, W. R.; Smith, P.; Tervoort, T. *Macromol Mater Eng* 2003, 288, 44.
23. Yamashita, A. *Plastics* 1997, 43, 47.
24. Kojima, Y.; Usuki, A.; Kawasumi, M.; Okada, A.; Fukushima, Y.; Kurauchi, T. *J Appl Polym Sci* 1993, 49, 1259.
25. Modesti, M.; Lorenzetti, A.; Bon, D.; Besco, S.; *Polymer* 2008, 30, 4602.
26. Wang, K.; Liang, S.; Deng, J.; Yang, H.; Zhang, Q.; Fu, Q.; Dong, X.; Wang, D.; Han, C. C. *Polymer* 2006, 47, 7131.
27. Deshmanea, C.; Yuana, Q.; Perkins, R. S.; Misra, R. D. K. *Mater Sci Eng A* 2007, 458, 150.
28. Fan, Q.; Yang, Y.; Ugbolue, S. C.; Wilson, A. R. National Textile Center, C01-D20 Annual Report, 2001–2004.
29. Dong, S. Y.; Bhattachary, D. *Composites A* 2007, 541.
30. Pozsgay, A.; Frater, T.; Papp, L.; Sajo I.; Pukanszky, B. *J Macromol Sci B Phys* 2002, 41, 1249.
31. Maiti, P.; Nam, P. H.; Okamoto, M.; Hasegawa, N.; Usuki, A. *Macromolecules* 2002, 35, 2042.
32. Xu, W.; Liang, G.; Zhai, H.; Tang, S.; Hang, G.; Pan, W. P. *Eur Polym J* 2003 39, 1467.
33. Dong, Y.; Bhattacharyy, D.; Hunter, P. J. *Comp Sci Technol* 2007, 5, 342.